AGU ADVANCING EARTH AND SPACE SCIENCE

Global Biogeochemical Cycles

RESEARCH ARTICLE
10.1029/2020GB006544

Lateral Particle Supply as a Key Vector in the Oceanic Carbon Cycle

Minkyoung Kim[1,2], Jeomshik Hwang[1], Timothy I. Eglinton[2], and Ellen R. M. Druffel[3]

[1]School of Earth and Environmental Sciences/Research Institute of Oceanography, Seoul National University, Seoul, South Korea, [2]Geological Institute, ETH Zürich, Zürich, Switzerland, [3]Department of Earth System Science, University of California, Irvine, Irvine, CA, USA

Key Points:

- Mean flux of lithogenic material accounts for 25 ± 20% of sinking particles globally
- Proportion and absolute flux of lithogenic material decreases with increasing distance from the seafloor and the coast
- Particulate organic carbon from sediment resuspension accounts for 0.2–0.7% of sinking particles and 4–11% of sinking POC

Supporting Information:

- Supporting Information S1
- Table S1

Correspondence to:
J. Hwang,
jeomshik@snu.ac.kr

Citation:
Kim, M., Hwang, J., Eglinton, T. I., & Druffel, E. R. M. (2020). Lateral particle supply as a key vector in the oceanic carbon cycle. *Global Biogeochemical Cycles*, *34*, e2020GB006544. https://doi.org/10.1029/2020GB006544

Received 14 JAN 2020
Accepted 18 AUG 2020
Accepted article online 24 AUG 2020

Abstract The export of particulate organic carbon (POC) from surface waters to the ocean interior via the biological carbon pump is largely envisioned as a vertical process. However, several lines of evidence suggest that lateral supply of aged organic matter hosted on lithogenic particles derived from sediment resuspension may also be a significant process. Despite its potential importance, lateral POC supply has not been systematically examined on a global scale. Here, we assess the contribution of resuspended sediment to sinking particulate matter in the ocean using literature data of sediment trap studies. Proportions and absolute fluxes of lithogenic material at 158 sites and available radiocarbon contents are compiled to develop a global-scale assessment. We find that lithogenic material accounts for 25 ± 20% of sinking particulate matter, comprising a mean flux of 67 mg $m^{-2}d^{-1}$. Lithogenic material flux generally decreased with increasing distance from the coast and with increasing height above the seafloor. The $\Delta^{14}C$ values of POC exhibited a linear relationship with a wt/wt ratio of lithogenic material to POC. Loadings of aged POC to lithogenic material obtained from this relationship were similar to or higher than POC content of the surface sediment in the vicinity. Based on this relationship, and the global mean of lithogenic material content of sinking particulate matter, we calculate that aged POC from sediment resuspension comprises 0.2–0.7% of sinking particles and 4–11% of sinking POC intercepted by sediment traps.

1. Introduction

The transport of carbon from surface waters to the deep ocean via primary production and subsequent export of particulate organic carbon (POC), known as the biological carbon pump, is a crucial process for sequestration of atmospheric CO_2 (Honjo et al., 2008; Volk & Hoffert, 1985). Sediment traps facilitate direct measurement of the POC flux to the ocean interior and have been widely used to understand the workings and magnitude of the biological pump (e.g., Honjo et al., 2008; Torres Valdés et al., 2014). In particular, large-scale studies such as Joint Global Ocean Flux Study (JGOFS) and Vertical Transport and Exchange (VERTEX) (e.g., Buesseler & Boyd, 2009; Dunbar et al., 1998; Honjo et al., 1995, 1999, 2000; Martin et al., 1987) have advanced our understanding of material fluxes to the ocean interior. For example, Honjo et al. (2008) undertook a global synthesis of sediment trap data, focusing on export to the mesopelagic/bathypelagic boundary and accompanying attenuation in biogeochemical fluxes during vertical transit from surface to deep waters. They found that the global annual flux of POC at a depth of 2,000 m was 120 mmol m^{-2} yr^{-1}, with similar fluxes for biogenic Si and inorganic carbon.

Hemipelagic sedimentation over continental margins involves both vertical and lateral particle transport, the latter involving translocation of lithogenic, or terrigenous, material (LM) from the coast to the ocean interior (Rea & Hovan, 1995). Strong currents prevalent in shallow continental margin settings promote sediment resuspension and lateral transport of resuspended particles (Bao et al., 2018; Hollister & Nowell, 1991; Hwang et al., 2010, 2017; Karakaş et al., 2006). Sediment resuspension, and associated entrainment of LM, or non-biogenic material, into sinking particles is not limited to continental margins (Honjo et al., 1982). Indeed, sediment resuspension appears to be a widespread phenomenon in the ocean (e.g., Gardner et al., 2018; Honda et al., 2000; Hwang et al., 2010; Nakatsuka et al., 1997; Sherrell et al., 1998), induced by a range of processes. Despite its prevalence, global-scale assessments of the influence of sediment resuspension and contributions from lateral supply of LM to sinking particles and sinking POC have yet not been systematically addressed.

With respect to POC, assessments of resuspended sediment contribution have been made based on radiocarbon measurements and organic molecular proxies (e.g., Hwang et al., 2005, 2009; Mollenhauer et al., 2003; Ohkouchi et al., 2002). Deep-ocean sinking POC frequently showed lower $\Delta^{14}C$ values (the fractionation-corrected value of $^{14}C/^{12}C$ relative to a standard; Broecker & Olson, 1959; Stuiver & Polach, 1977) than expected when freshly produced POC was considered as the only source (Hwang et al., 2010). The $\Delta^{14}C$ value of sinking POC serves as an effective tracer of resuspended sedimentary POC because of the contrast in $\Delta^{14}C$ values between fresh POC and sedimentary POC (Hwang et al., 2004), and this contrast has been used in two end-member isotopic mass balance calculations to estimate that resuspended sedimentary POC accounts for ~30% of sinking POC (Hwang et al., 2010).

Sediments are enriched in clay and silt (Gardner et al., 1985; Walsh et al., 1988). Al (aluminum) is a major constituent of aluminosilicate minerals. The Al content of the continental crust is relatively uniform globally (8.23% on average; Taylor & McLennan, 1985). Hence, Al contents can serve as a general tracer of LM. Since eolian input is usually much less significant than resuspended sediments in terms of particulate Al supply to the water column (Duce et al., 1991; Hwang et al., 2010), and scavenging of dissolved Al to sinking particles is also of minor importance (Lam et al., 2015), Al provides a tracer of resuspended sediment particles. The $\Delta^{14}C$ and Al contents of sinking particles showed a strong negative correlation, implying that aged POC is associated with LM (Hwang et al., 2010).

In this paper, we compiled literature data to develop a global-scale assessment of contributions of LM to sinking particulate matter. We find that these contributions are significant in various oceanic settings, particularly over continental margins. Examination of $\Delta^{14}C$ values of sinking POC revealed strong relationships with parameters that represent contribution of resuspended sediment. We then derive estimates for the contribution of aged POC from sediment resuspension to sinking POC based on these relationships and global LM flux data.

2. Data

We used literature data derived from sediment trap studies (supporting information Table S1). The majority of data were obtained from a JGOFS website (http://usjgofs.whoi.edu/mzweb/data/Honjo/sed_traps.html; data compiled by S. Honjo, R. Francois, and S. J. Manganini), with additional data obtained from the PANGAEA website (https://www.pangaea.de/) and from individual papers not included in the above mentioned data compilations (e.g., Hwang et al., 2015, 2017; Kim et al., 2015, 2017, 2019; Torres Valdés et al., 2014).

For compilation of the proportions and absolute fluxes of LM, priority was given in the following order: If LM data were explicitly presented in the original literature, the data were adopted as reported (e.g., Dunbar et al., 1998; Kawahata, 2002; Kawahata et al., 1998, 2000; Kempe & Knaack, 1996). Most of the studies did not report the proportion of LM explicitly, so the latter was estimated as the difference between the total particle mass and the sum of biogenic components (i.e., opal, $CaCO_3$, and particulate organic matter $= 1.88 \times$ POC; the ratio between organic matter and POC from Lam et al., 2011); this was called the "unaccounted-for" fraction. When an estimated value was negative, or data were not available for all three biogenic components, the proportion of LM was calculated using the Al content (Al content $\times$ 12.15, Taylor & McLennan, 1985). The unaccounted-for fraction and the LM based on Al content showed a reasonably good correlation ($y = (1.141 \pm 0.018) \times x + (2.93 \pm 0.30)$, $r = 0.77$, $n = 1933$; here x and y represent Al-based proportion of LM and unaccounted-for fraction, respectively; Figure S1). Considerable discrepancies between the two fractions were observed for those samples with low LM fluxes (Figure S1). Results of very low Al-derived values with high unaccounted-for fraction values were mostly from the Southern Ocean (e.g., JGOFS data from Collier et al., 2000).

$\Delta^{14}C$ values of sinking POC were obtained from individual papers. $\Delta^{14}C$ values of suspended POC and dissolved inorganic carbon in surface waters and surface sediments at or proximal to sediment trap sites were also obtained from individual papers (Table 1).

10.1029/2020GB006544

Table 1
Intercept and Slope Values of the Linear Trend Lines Between the Observed $\Delta^{14}C$ Values and the Ratio of Lithogenic Material to POC and α Values at Each Site (Figure 5). $\Delta^{14}C$ of fresh biogenic particles and properties of surface sediment at six locations are also listed

Site (St. #) ($\Delta^{14}C$ data source)	Water depth (m)	Trap depths (m)	Linear trend line: Intercept	Linear trend line: Slope	Linear trend line: (R^2, # of data)	$\alpha \times 100$	$\Delta^{14}C$ (‰) of fresh biogenic particles[a]	Surface sediments: $\Delta^{14}C$ (‰)	Surface sediments: Al (%)	Surface sediments: OC (%)	Surface sediments: OC/ (Al × 12.15) × 100
Canada Basin, Arctic (#149, 151, 154) (Hwang et al., 2015)	3,824	2,050 3,100 3,750	−60 ± 12	−8.2 ± 0.5	(0.58, 177)	1.2 ± 0.1	+20 (Jones et al., 1994)	−720 ± 118[b] (Goñi et al., 2013)	7.73 (Hwang et al., 2015)	1.3 (Goñi et al., 2013)	1.4
St. MS, NW East/Japan Sea (#110) (Otosaka et al., 2008)	3,600	1,000 3,000	+9.8 ± 10	−9.3 ± 1.3	(0.59, 63)	2.6 ± 0.4	+56 ± 26 (Otosaka et al., 2008)	−375 ± 3 (Otosaka et al., 2008)	9.0 (Otosaka et al., 2004)	1 (Niino et al., 1969)	0.9
St. M, NE Pacific (#95) (Hwang et al., 2010)	4,100	3,450	+58 ± 15	−9.7 ± 2.3	(0.45, 22)	3.0 ± 0.8	+60 (Masiello et al., 1998)	−266 ± 11 (Wang et al., 1998)	9.5 (Goldberg & Arrhenius,, 1958)	1.4 (Wang et al., 1998)	1.2
Amundsen Sea, Antarctic (#8) (Kim et al., 2015)	530	400	−170 ± 5	−3.8 ± 0.7	(0.54, 23)	1.6 ± 0.4	−153 (Kim et al., 2016)	−418 (Kim et al., 2016)	7.4 (Kim & Hwang, unpub. data)	1.0 (Kim et al., 2015)	1.1
Okinawa Trough, NW Pacific (#82) (Honda et al., 2000)	1,650	1,000 1,500	+49 ± 18	−3.3 ± 0.9	(0.73, 6)	1.0 ± 0.3	+105 (Honda et al., 2000)	−300[c] (Honda et al., 2000)	8.2 ± 1.3 (Hsu et al., 2003)	1.0 ± 0.5 (Honda et al., 1997, 2000; Kennicutt et al., 1987)	1.0
St. W, NW Atlantic (#106) (Hwang et al., 2017)	3,050	1,000 2,000 3,000	+25 ± 3	−4.0 ± 0.3	(0.64, 111)	1.4 ± 0.3	+58 ± 7 (Hwang et al., 2009)	−260 (Griffith et al., 2010; Hwang et al., 2017)	6.9 (Gardner et al., 1985)	0.82 ± 0.16[d]	1.0

[a]$\Delta^{14}C$ (‰) of fresh biogenic particles are the values of either suspended POC or dissolved inorganic carbon in the surface water (see each reference for more details). [b]$\Delta^{14}C$ values of sediments from the Beaufort Sea slope, Barrow Canyon, and Mackenzie Shelf ranged between −521‰ and −877‰ (Goñi et al., 2013). The average value of the Mackenzie Shelf (−720 ± 118‰) was chosen. [c]From −330‰ at the center of the East China Sea to −60‰ toward continental slope with increasing water depth from 80 to 1,000 m (Honda et al., 2000). We used −300‰ for sediment end-member, considering possible input of the lateral transport of aged sediment into the Okinawa trough from the continental slope (Honda et al., 2000) and Taiwanese river (Liu et al., 2008). [d]An average value of 0–1 cm core-top sediments at four locations on the New England Slope (Hwang and Eglinton, unpublished data, 2006).

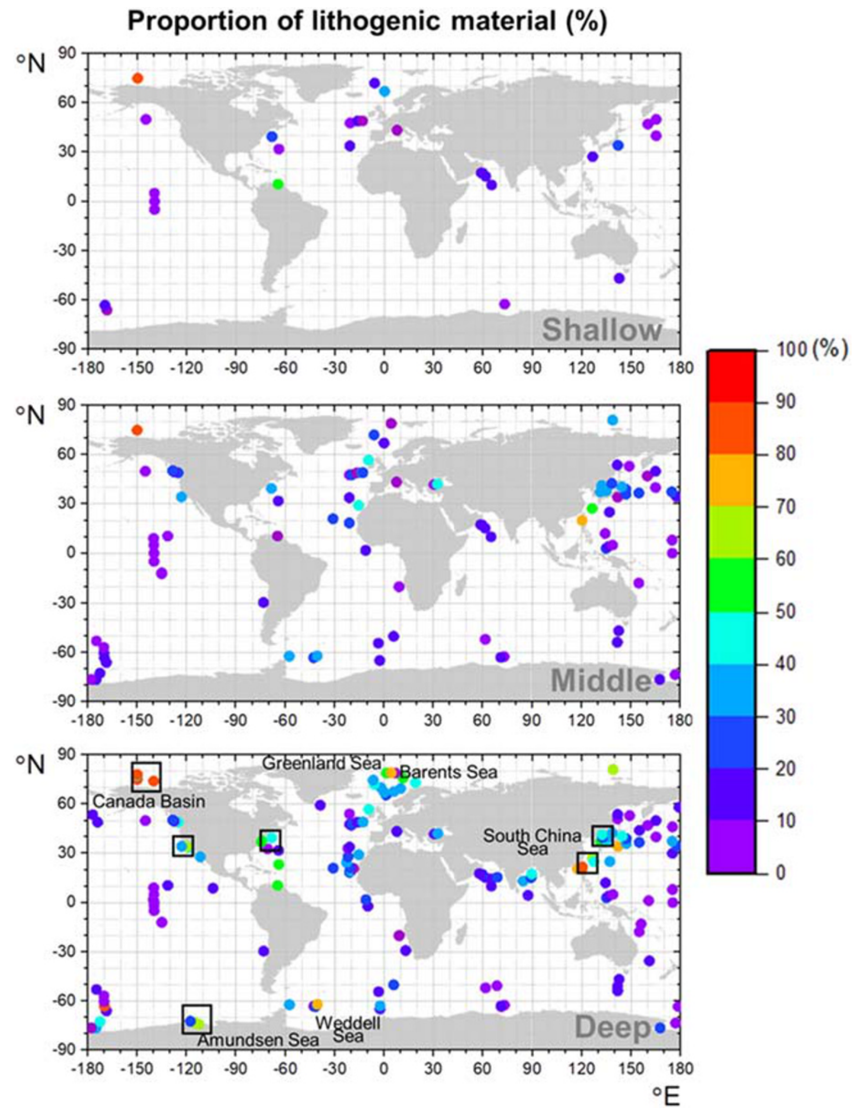

Figure 1. Proportion of lithogenic material (%) in sinking particulate matter at each study site. Each symbol represents the arithmetic mean of the values observed at various times at the same location. When data exist only at one depth at a site, they are presented as deep samples. When data exist at more than one depth at a site, the data are presented in three "relative" trap depth bins (i.e., shallow, middle, and deep trap depths). Symbols within the rectangles indicate the sites for which radiocarbon isotope results are presented in Figure 5. For interpretation of the color coding of the symbols, the reader is referred to the web version of this article.

3. Results

3.1. Proportion and Absolute Flux of Lithogenic Material in Sinking Particles

The compiled data (a total of 7,792 data points from 158 sites) clearly show that LM accounts for a significant fraction of sinking particulate matter globally (Figure 1 and Table S1). An arithmetic mean of the average proportion of LM at each sampling site was 25 ± 20% of the sinking particulate mass (Figure 1). Low proportions of LM (i.e., <10%) were mainly observed in open ocean settings. In the Southern Ocean, the proportion of LM was ~20%. Continental margin sites, including the northeast/northwest Pacific and the northeast/northwest Atlantic showed higher values (~30%). High values were also observed in the Atlantic Nordic-Norwegian Sea, the Greenland Sea, and the Barents Sea. In the Amundsen Sea and the

10.1029/2020GB006544

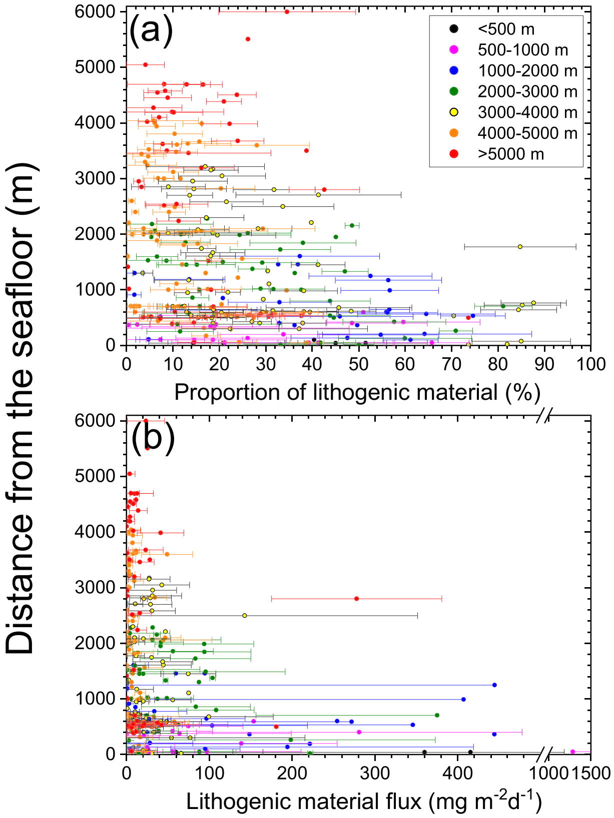

Figure 2. (a) Proportion of lithogenic material (%) and (b) lithogenic material flux (mg $m^{-2}d^{-1}$) against the distance from the seafloor. Color coding denotes total water depth (m) of each sampling site. The symbol and horizontal line of each time-series data set indicate the arithmetic mean and the standard deviation of the data. The maximum lithogenic material flux is 5,500 mg $m^{-2}d^{-1}$ and is not shown here (also note the axis-break). For interpretation of the references to color in this figure legend, the reader is referred to the web version of this article.

Weddell Sea, the mean proportion of LM was ~50%. Extremely high values (>80%) were observed in the Arctic Canada Basin.

Absolute LM flux ranged from near zero to 5,500 mg $m^{-2}d^{-1}$ (Figure S2). The arithmetic mean of the average LM flux for all sites and all water depths was 67 mg $m^{-2}d^{-1}$ (Table S1). Values greater than the mean were mainly observed on the continental margins (Figure S2b). In the Arctic Canada Basin the flux was very low despite very high proportions of LM to overall flux. Relatively high fluxes were observed in most margin sites of the northeastern Pacific, in the northwest Atlantic, as well as around Antarctica including the Ross Sea, the Amundsen Sea, and the Antarctic Peninsula.

In general, the proportion of LM decreased with increasing height above the seafloor (Figure 2a). Values >50% were observed in sinking particles intercepted within 2,000 m above the seafloor and particularly within ~1,000 m of the seafloor. Correspondingly, proportions of LM were high for those sites where total water depths were less than 1,000 m (black and magenta symbols in Figure 2a). However, the proportion of LM was significant above this layer as well, and even at 4,000 m above the seafloor, with observed values ranging from 20% to 40% of sinking particulate matter. Abnormally high values, 35% on average, at 6,000 m above the seafloor (a water depth of 1,000 m) were observed in the northern Japan Trench (Shin et al., 2002). Globally, LM accounts for 34 ± 16%, 33 ± 21%, and 20 ± 19% of sinking particulate matter over the continental shelf (<500 m), slope (500–3,000 m), and abyssal plain (>3,000 m), respectively.

Absolute LM flux also showed vertical attenuation with increasing distance above the seafloor (Figure 2b). High LM fluxes (>200 mg $m^{-2}d^{-1}$) were observed mainly within ~1,300 m from the seafloor. At a given depth and location, the ranges of proportions and absolute fluxes of LM (1 standard deviation error bars, Figures 2 and S3) were large, indicating sporadic rather than continuous supply of LM. The proportion and absolute flux of LM also showed attenuation with increasing distance from the coast (Figure S3), with LM fluxes <30 mg $m^{-2}d^{-1}$ for distances >2,200 km.

We examined LM flux at all 25 sites where the flux was measured at more than two depths simultaneously (Figure 3). The vertical distribution of LM flux can mostly be grouped into five categories: (i) similar LM fluxes at all depths, (ii) increasing flux with increasing depth, (iii) minimum flux at mid-depth, (iv) maximum flux at mid-depth, and (v) decreasing flux with increasing depth. The global feature of decreasing LM flux with increasing height above the seafloor was not always observed at each examined site. The mean fluxes at most sites were lower than 70 mg $m^{-2}d^{-1}$, because the majority were open ocean sites with total water depths mostly greater than 3,000 m. The first category (similar fluxes at all depths) includes two cases, in Prydz Bay, Antarctica (#11) and the Arabian Sea (#55). Absolute LM flux was low (<10 mg $m^{-2}d^{-1}$) at both sites. The second category, characterized by increasing flux with increasing depth (10 sites, #62, 65, 88, 92, 93, 106, 116, 125, 147, and 151), was the most frequent pattern observed. Four sites exhibited a minimum flux at mid-depth (#51, 119, 131, and 143). Most stations with maximum flux at mid-depth (eight sites, #30, 42, 66, 82, 108, 115, 120, and 130) were located adjacent to continent shelves where particles may be exported from the continental shelf and slope, potentially as nepheloid layers moving along isopycnal surfaces (McCave et al., 2001). As an exception, decreasing LM flux with increasing water depth was observed in the Cariaco Basin (#56). Although the reason for this observation is not clearly stated by the authors, earthquake-induced supply of resuspended sediment from the slope (Thunell et al., 1999) or riverine supply of LM from the Venezuelan coastline may be responsible (Thunell et al., 2007).

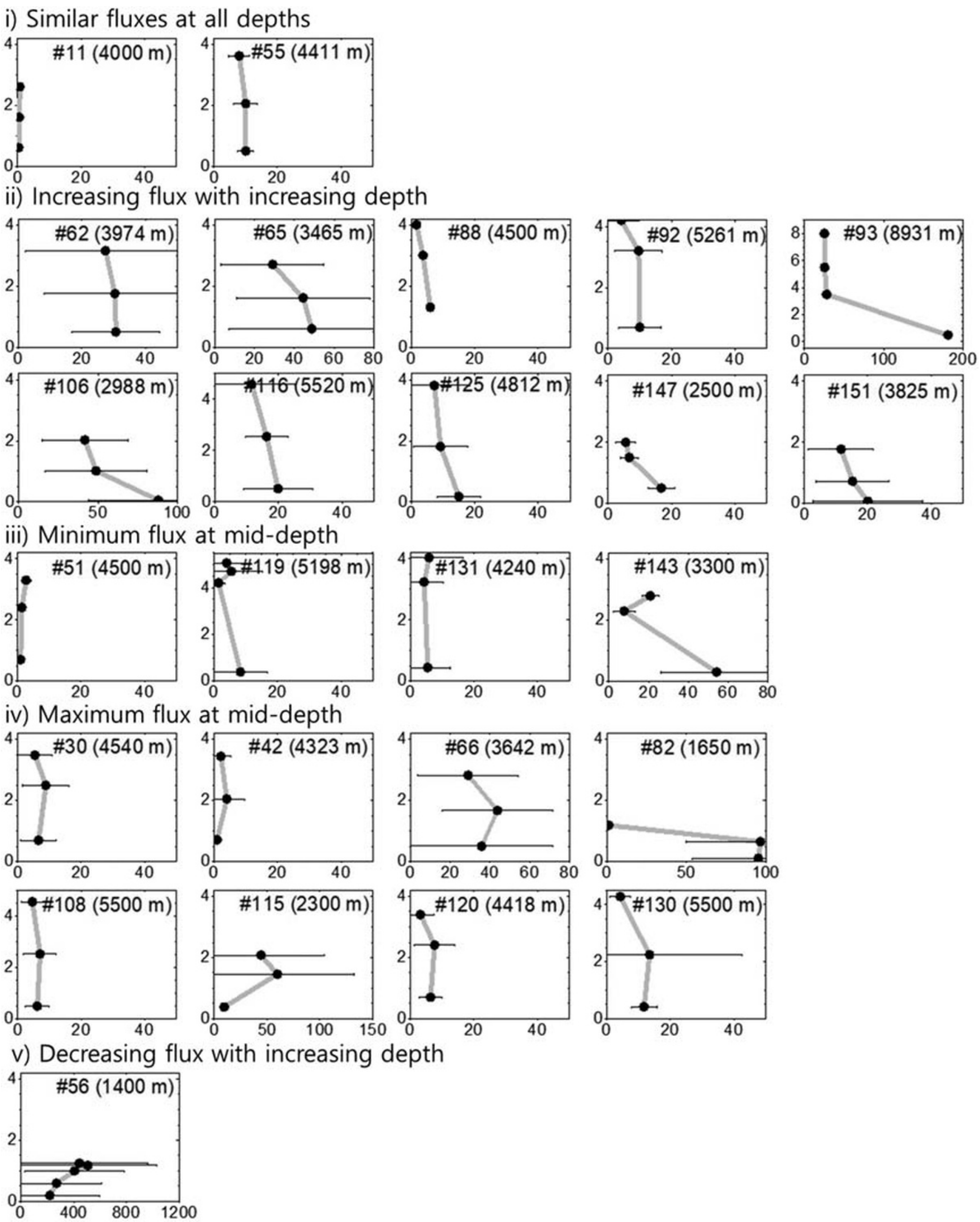

Figure 3. Vertical distribution of lithogenic material flux at 25 sites where simultaneous measurements at more than two depths are available. The *y*-axis is the height above the seafloor in km. The station number (Table S1) and total water depth (in parenthesis) are indicated for each plot. Symbols and horizontal lines indicate mean values and standard deviations of each data set. Note that *x*-axis scales are not the same for all plots.

4. Discussion

4.1. Vertical and Horizontal Variation of Resuspended Sediment Contributions to Sinking Particulate Matter

In general, regions of high LM flux, such as the Atlantic-Nordic Sea and the northwest Atlantic margin, match the regions of high particulate matter concentration in the bottom waters (i.e., 10 m above bottom)

10.1029/2020GB006544

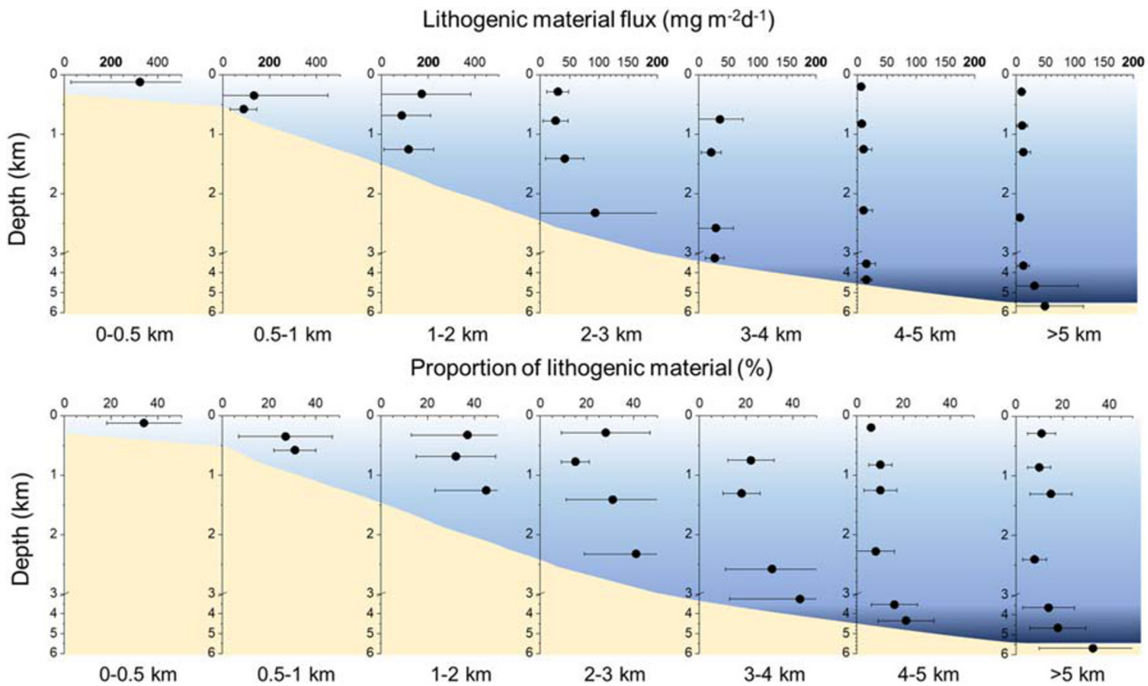

Figure 4. Average and standard deviation of lithogenic material flux in mg $m^{-2}d^{-1}$ (upper panel) and proportion of lithogenic material in % (lower panel) plotted against sample collection depth (averaged for each sampling depth bin). Data were grouped into 7 "sediment trap deployment depth" bins (0–0.5 km, 0.5–1 km, 1–2 km, 2–3 km, 3–4 km, 4–5 km, and >5 km). Data are presented in 7 "total water depth" bins: from left to right, 0–0.5 km, 0.5–1 km, 1–2 km, 2–3 km, 3–4 km, 4–5 km, and >5 km. Note the difference in *x*-axis scales for lithogenic material flux between plots for total water depths of 0–2 km versus >2 km. Also note the break in *y*-axis scale. The bathymetry in the background is not to scale.

based on transmissometry surveys (Figure 3 in Gardner et al., 2018). Although the data overlap between this transmissometry study (Gardner et al., 2018) and the sediment trap locations used in our study are insufficient to allow direct comparisons, the high proportions and absolute fluxes of LM near the seafloor clearly indicate that sediment resuspension is a major source of LM.

When the LM flux data are binned into seven groups according to total water depth and sampling depth (i.e., 0–500, 500–1,000, 1,000–2,000, 2,000–3,000, 3,000–4,000, 4,000–5,000, and >5,000 m), several features of LM supply from the near-surface sources and near-seafloor sources emerge (Figure 4 and Tables 2, S2, and S3). LM flux was distinctly higher on the continental shelf than other environments. Over the upper continental slope (500–1,000 m water depth), LM flux was higher at shallower depths than near the seafloor, demonstrating the importance of resuspended sediment particles emanating from the shelf/slope break.

Table 2
Mean Contribution (%) of Aged POC to Total Particulate Matter and Sinking POC (in Parenthesis) at Each "Sample Collection Depth" Bin at Each "Total Water Depth" Bin. These estimates were obtained under the assumption of α = 1

	Total water depth (m)						
Trap depth	<500 m	500–1,000 m	1,000–2,000 m	2,000–3,000 m	3,000–4,000 m	4,000–5,000 m	>5,000 m
<500 m	0.3 (2.4)	0.3 (2.8)	0.4 (4.6)	0.3 (2.8)	no data	0.1 (0.5)	0.1 (1.2)
500–1,000 m		0.3 (4.0)	0.3 (3.4)	0.2 (2.1)	0.2 (2.5)	0.1 (1.1)	0.1 (1.7)
1,000–2,000 m			0.5 (8.2)	0.3 (4.3)	0.2 (2.5)	0.1 (1.4)	0.2 (2.1)
2,000–3,000 m				0.4 (9.5)	0.3 (5.6)	0.1 (1.6)	0.1 (1.6)
3,000–4,000 m					0.4 (9.7)	0.2 (3.0)	0.1 (3.8)
4,000–5,000 m						0.2 (3.8)	0.2 (3.9)
>5,000 m							0.3 (8.0)
Column average	0.3 (2.4)	0.3 (3.4)	0.4 (5.4)	0.3 (4.7)	0.3 (5.1)	0.1 (1.9)	0.2 (3.2)

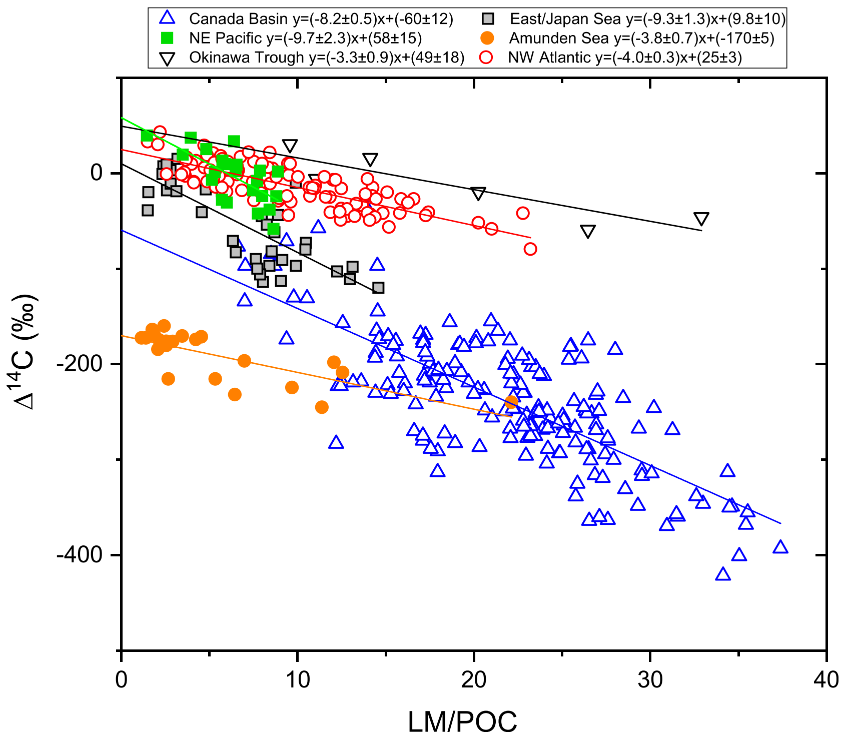

Figure 5. Relationship between $\Delta^{14}C$ value of sinking POC and the ratio of lithogenic material to POC (LM/POC) in sinking particulate matter. Intercepts and slopes of the linear fit lines for each site are shown in the legend.

This observation is consistent with the prevalence of intermediate nepheloid layers observed over the continental slopes (Karakaş et al., 2006; Lorenzoni et al., 2009; McCave et al., 2001). In the 1,000–2,000 m water depth bin, a clear water layer is evident between the surface and near the seafloor, while in the 2,000–3,000 m depth bin, local sediment resuspension and/or lateral transport along the slope appeared more important than the particles emanating from the shelf break. From depth bins greater than 3,000 m, the vertical distribution of LM flux was uniform, and no significant elevation in LM flux was observed near the seafloor, with overall LM fluxes diminishing with increasing distance from the coast. Exceptionally, a distinct near-seafloor elevation in LM flux observed in the 5,000–6,000 m bin was driven by high LM fluxes at the Japan Trench site.

The proportion of LM in sinking particulate matter exhibits slightly different features to those for absolute LM flux (Figure 4). This is because the proportion of LM in sinking particulate matter is affected by absolute flux of biogenic material, with the latter decreasing as a consequence of decomposition and dissolution of biogenic particles during their vertical descent. In particular, for the 3,000–4,000 and 4,000–5,000 m water depths, increases in the proportion of LM toward the seafloor were clearly observed, whereas LM flux remained uniform or increased only slightly.

4.2. Insights From Radiocarbon Analysis

Hwang et al. (2010) showed that $\Delta^{14}C$ values of POC were negatively correlated with Al content of sinking particles. This correlation was interpreted as indicating that the major source of aged POC was resuspended sediment and that aged POC was tightly associated with aluminosilicate minerals. We have expanded the data set by adding data published since Hwang et al. (2010). As in Hwang et al. (2010), we modeled the composition of sinking particles as a mixture between vertically transported fresh biogenic particles and particles resuspended from surface sediment, focusing on POC and LM. Eolian input of LM was not considered in this model.

The $\Delta^{14}C$ value was compared to the wt/wt ratio of LM to POC of sinking particles (hereafter LM/POC) at six locations where both $\Delta^{14}C$ values of sinking POC and Al content data are available (Figure 5). These sites represent various oceanic environments including an ice-covered continental shelf (Amundsen Sea), a marginal sea with deep basins (East/Japan Sea), an abyssal site (Station M), a continental slope location (Station W), a seasonally ice-covered Arctic Ocean basin (Canada Basin), and a deep-ocean trough (Okinawa Trough). The $\Delta^{14}C$ and LM/POC values at each site showed significant linear relationships (Figure 5). The Arctic Canada Basin data showed the widest range of both $\Delta^{14}C$ values and LM/POC. A very different relationship was observed for the sediment trap samples from the northern South China Sea (not shown; Blattmann et al., 2018). This is likely attributed to exceptionally large inputs of fossil (petrogenic) POC from bedrock erosion on Taiwan as well as selective removal of organic matter depending on the mineralogy of the LM (Blattmann et al., 2019). Therefore, these results are not discussed further in this paper.

We used a two end-member mixing model to assess the underlying reason for the apparent linear relationship between observed $\Delta^{14}C$ values and LM/POC evident in Figure 5. In the mixing model, sinking POC is a mixture between fresh POC (POC_{fresh} with $\Delta^{14}C_{fresh}$) and aged POC derived from sediment resuspension (POC_{resusp} with $\Delta^{14}C_{resusp}$). POC_{resusp} was set to be proportional to LM of sinking particle samples (all data for the proportions of LM used in this section were based on Al content) under the assumption that POC_{resusp} is tightly associated with LM, that is,

$$POC_{resusp} = LM \times \alpha \tag{1}$$

where α is a proportionality constant. Also,

$$\Delta^{14}C_{observed} = \Delta^{14}C_{fresh} \times (1 - f) + \Delta^{14}C_{resusp} \times f \tag{2}$$

where f is the fraction of POC_{resusp} in total POC (here and in equation 3, POC = POC_{fresh} + POC_{resusp}) in the two end-member mixing model. Then the relationship between the observed $\Delta^{14}C$ values and LM/POC is as follows.

$$\Delta^{14}C_{observed} = \left[\alpha \times \left(\Delta^{14}C_{resusp} - \Delta^{14}C_{fresh}\right)\right] \times LM/POC + \Delta^{14}C_{fresh} \tag{3}$$

Derivation of the equation is presented in the supporting information. If the relationship is linear, $\alpha \times (\Delta^{14}C_{resusp} - \Delta^{14}C_{fresh})$ is equivalent to the slope of the line, and $\Delta^{14}C_{fresh}$ is equivalent to the intercept. The slope of each linear regression ranged between −3.3 and −10.2 (Figure 5 and Table 1). The linear relationship suggests that if the $\Delta^{14}C$ values of the two end-members are fixed, α is constant at a given site. Therefore, α, the proportion of aged POC to LM, does not appear to be altered significantly in the water column.

There are several advantages in using the ratio of LM/POC instead of Al content for comparison with $\Delta^{14}C$ values of sinking POC. First, the relationship appears to be linear instead of having a convex upward curvature and therefore is easier to derive a trend line (Figure 5). Second, the properties of the fresh particle end-member do not need to be preassigned since $\Delta^{14}C_{fresh}$ can be obtained from the y-intercept of linear fit of the data (Figure 5). Third, and most importantly, the relationship can be treated analytically. Although both the α value and the difference between $\Delta^{14}C_{resusp}$ and $\Delta^{14}C_{fresh}$ cannot be determined independently, if one of the two values is known, the other value can be calculated from the slope of the linear trend line.

Because the α value is the ratio of sediment-derived aged POC to LM (also mainly derived from sediment) in sinking particles, comparison of α values with OC (organic carbon) to LM ratios in the proximal surface sediment may provide information on whether association of OC with clay minerals is altered during the process of resuspension and subsequent transport in the water column. We used $\Delta^{14}C$ values of proximal surface sediment for $\Delta^{14}C_{resusp}$, the y-intercept values for $\Delta^{14}C_{fresh}$, and the line slope to estimate the α values. Resulting estimates of α (in %) ranged between 1.0 and 3.0 (Table 1). The ratio of OC to LM in the surface sediments ranged between 0.9% and 1.4% (Table 1), similar to or smaller than the α values. In this calculation, we simply used Al content to estimate the LM content in sediments. In some cases, however, this returns an LM content of >100%, indicating that Al to LM ratios vary spatially and should be used with caution. Further regional correction depending on the mineralogy of the local LM is therefore warranted (e.g., Tagliabue et al., 2019 for the South Pacific). Although the uncertainty for the estimated α values is potentially large, the similarity between α values and OC to LM ratios of surface sediments suggests that the association of aged OC with LM is not greatly altered during the resuspension process.

4.3. Contribution of Aged POC to Sinking Particles in the Ocean

Based on the above relationships between the proportion of aged POC and LM content, we can use the more comprehensive data available for the latter to estimate the contribution of aged POC to sinking particulate matter. Because we use the $\Delta^{14}C$ values of the surface sediment to obtain α values, these estimates do not include any rebounded particles ("those particles that have reached the sediment surface but have not become incorporated into the sediments," Walsh et al., 1988), or fluffy aggregates, which would be rather fresh (higher $\Delta^{14}C$ values; Wang et al., 1998) and lead to an underestimation of the actual contribution of resuspended POC.

Using an α value of 1% and compiled data on the proportion of LM in sinking particulate matter, we estimate that aged POC accounts for 0.2% (±0.1) of sinking particulate matter and 3.6% (±2.5) of sinking POC globally (Table 2). In general, the contribution of aged POC to sinking POC increased with increasing trap depth, with a mid-depth minimum in the 1,000–3,000 m range, similar to the proportion of LM. Higher values (8–10%) were observed near the seafloor on the continental slope (station depths of 1,000–4,000 m), and the lowest value was observed for particles intercepted at shallow depths in the open ocean (4,000–5,000 m). The contribution of aged POC to sinking POC averaged over the water column increased from the shelf (2.4–3.4%) toward the slope (4.7–5.1%) then decreased toward the abyssal plain (1.9–3.2%). The spatial variation is attributed to the relative strength of the fluxes of fresh POC and aged POC in each region. Aged POC contributions were highest near the seafloor (6.5% when the total water depth and trap depth were in the same bin) and exhibited a general decrease from almost 4% to slightly more than 1% as the difference between the trap depth and water depth increased from <500 to >4,500 m (Table 2).

A major source of uncertainty in the above estimates is the range of α values. If the true α was 3% instead of 1% then aged POC contributions would increase threefold (i.e., to global values of 0.7% and 11% of sinking particulate matter and sinking POC, respectively). However, more extensive $\Delta^{14}C$ data sets for sinking POC from various oceanographic settings are needed to better constrain the α values. Furthermore, spatial and temporal variability in the sources of resuspended particles and their biogeochemical properties, as well as $\Delta^{14}C$ values and LM contents and compositions of surface sediments, are necessary to develop a more comprehensive assessment of the influence of sediment resuspension and lateral particle supply on the oceanic carbon cycle. Nevertheless, our results show that sediment resuspension and contributions of aged POC to sinking particulate matter should be considered in at least two aspects of biological pump studies using sediment traps: (1) Where aged POC supplied from sediment resuspension is locally high, caution should be taken in quantification of vertical flux based on the observed POC flux; and (2) measurements of Al content in sinking particulate matter are recommended for quantitative assessment of the contribution of resuspended sediment, and associated aged POC, to sinking particles.

5. Summary

Compiled data from sediment trap studies show that LM (or non-biogenic material) comprises a significant fraction of sinking particulate matter in the oceans. The proportion of LM decreased with increasing distance from the coast and above the seafloor. Globally, LM accounts for 34 ± 16%, 33 ± 21%, and 20 ± 19% of the sinking particulate matter over the continental shelf (<500 m), slope (500–3,000 m), and abyssal plain (>3,000 m), respectively. The vertical distribution of LM in shelf waters to 3,000 m water depth suggests input from both intermediate nepheloid layers and benthic nepheloid layers. At water depths greater than 3,000 m, LM flux was low and more uniformly distributed throughout the water column.

A linear relationship is apparent between $\Delta^{14}C$ values of POC and the abundance ratio of LM/POC in sinking particulate matter. Based on this relationship and the $\Delta^{14}C$ values of the surface sediment OC, aged POC loading on LM was estimated to be ~1.0% but potentially as high as 3.0%. Using this estimate and a compilation of data on the proportion of LM, we find that aged POC accounts for 0.2–0.7% of sinking particulate matter and 4–11% of sinking POC globally. Lateral supply of resuspended sediment to sinking particles should thus be considered in developing a comprehensive understanding of oceanic particle flux and carbon cycling.

Conflict of Interest

The authors declare no financial conflicts of interest.

Data Availability Statement

The data used in this study can be obtained from Table S1 in the supporting information. Table S1 is also archived at the National Oceanic and Atmospheric Administration's National Centers for Environmental Information (NCEI) web interface (https://accession.nodc.noaa.gov/0210959).

Acknowledgments

This research was partly supported by the National Research Foundation of Korea (NRF) grant funded by the Korean Government (2020R1A2C1008378). M. Kim was partly supported by the National Research Foundation of Korea grant funded by the Korean Government (Global PhD fellowship NRF-2015H1A2A1032018) and the Young Researchers' Exchange Programme between Korea and Switzerland 2017–2018 (NRF-2017K1A3A1A14092122).

References

Bao, R., van der Voort, T. S., Zhao, M., Guo, X., Montluçon, D. B., McIntyre, C., & Eglinton, T. I. (2018). Influence of hydrodynamic processes on the fate of sedimentary organic matter on continental margins. *Global Biogeochemical Cycles*, *32*, 1420–1432.

Blattmann, T., Liu, Z., Zhang, Y., Zhao, Y., Haghipour, N., Montluçon, D. B., et al. (2019). Mineralogical control on the fate of continentally derived organic matter in the ocean. *Science*, *366*, 742–745.

Blattmann, T. M., Zhang, Y., Zhao, Y., Wen, K., Lin, S., Li, J., et al. (2018). Contrasting fates of petrogenic and biospheric carbon in the South China Sea. *Geophysical of Research Letters*, *45*, 9077–9086.

Broecker, W. S., & Olson, E. A. (1959). Lamont radiocarbon measurements VI. *American Journal of Science*, *1*, 111–132.

Buesseler, K. O., & Boyd, P. W. (2009). Shedding light on processes that control particle export and flux attenuation in the twilight zone of the open ocean. *Limnology and Oceanography*, *54*, 1210–1232.

Collier, R., Dymond, J., Honjo, S., Manganini, S., Francois, R., & Dunbar, R. (2000). The vertical flux of biogenic and lithogenic material in the Ross Sea: Moored sediment trap observations 1996–1998. *Deep-Sea Research Part II*, *47*, 3491–3520.

Duce, R., Liss, P., Merrill, J., Atlas, E., Buat-Menard, P., Hicks, B., et al. (1991). The atmospheric input of trace species to the world ocean. *Global Biogeochemical Cycles*, *5*(3), 193–259.

Dunbar, R. B., Leventer, A. R., & Mucciarone, D. A. (1998). Water column sediment fluxes in the Ross Sea, Antarctica: Atmospheric and sea ice forcing. *Journal of Geophysical Research*, *103*, 30,741–30,759.

Gardner, W. D., Richardson, M. J., & Mishonov, A. V. (2018). Global assessment of benthic nepheloid layers and linkage with upper ocean dynamics. *Earth and Planetary Science Letters*, *482*, 126–134.

Gardner, W. D., Southard, J. B., & Hollister, C. D. (1985). Sedimentation, resuspension and chemistry of particles in the northwest Atlantic. *Marine Geology*, *65*, 199–242.

Goldberg, E. D., & Arrhenius, G. O. S. (1958). Chemistry of Pacific pelagic sediments. *Geochimica et Cosmochimica Acta*, *13*(2–3), 153–212.

Goñi, M. A., O'Connor, A. E., Kuzyk, Z. Z., Yunker, M. B., Gobeil, C., & Macdonald, R. W. (2013). Distribution and sources of organic matter in surface marine sediments across the North American Arctic margin. *Journal of Geophysical Research: Oceans*, *118*, 4017–4035.

Griffith, D. R., Martin, W. R., & Eglinton, T. I. (2010). The radiocarbon age of organic carbon in marine surface sediments. *Geochimica et Cosmochimica Acta*, *74*, 6788–6800.

Hollister, C., & Nowell, A. (1991). Prologue: Abyssal storms as a global geologic process. *Marine Geology*, *99*, 275–280.

Honda, M., Kusakabe, M., Nakabayashi, S., & Tanaka, T. (1997). Sediment trap experiment in the Okinawa Trough: Behavior of lithogenic material in the Okinawa trough and its biogeochemical characteristics. *Jamstecr*, *36*, 9–52.

Honda, M. C., Kusakabe, M., Nakabayashi, S., & Katagiri, M. (2000). Radiocarbon of sediment trap samples from the Okinawa trough: Lateral transport of ^{14}C-poor sediment from the continental slope. *Marine Chemistry*, *68*, 231–247.

Honjo, S., Dymond, J., Collier, R., & Manganini, S. J. (1995). Export production of particles to the interior of the equatorial Pacific Ocean during the 1992 EqPac experiment. *Deep-Sea Research Part II*, *42*, 831–870.

Honjo, S., Dymond, J., Prell, W., & Ittekkot, V. (1999). Monsoon-controlled export fluxes to the interior of the Arabian Sea. *Deep-Sea Research Part II*, *46*, 1859–1902.

Honjo, S., Francois, R., Manganini, S., Dymond, J., & Collier, R. (2000). Particle fluxes to the interior of the Southern Ocean in the Western Pacific sector along 170 °W. *Deep-Sea Research Part II*, *47*, 3521–3548.

Honjo, S., Manganini, S. J., Krishfield, R. A., & Francois, R. (2008). Particulate organic carbon fluxes to the ocean interior and factors controlling the biological pump: A synthesis of global sediment trap programs since 1983. *Progress in Oceanography*, *76*, 217–285.

Honjo, S., Manganini, S. J., & Poppe, L. J. (1982). Sedimentation of lithogenic particles in the deep ocean. *Marine Geology*, *50*, 199–220.

Hsu, S.-C., Lin, F.-J., Jeng, W.-L., Chung, Y.-c., & Shaw, L.-M. (2003). Hydrothermal signatures in the southern Okinawa Trough detected by the sequential extraction of settling particles. *Marine Chemistry*, *84*(1–2), 49–66.

Hwang, J., Druffel, E. R., Griffin, S., Smith, K. L., Baldwin, R. J., & Bauer, J. E. (2004). Temporal variability of Δ^{14}C, δ^{13}C, and C/N in sinking particulate organic matter at a deep time series station in the northeast Pacific Ocean. *Global Biogeochemical Cycles*, *18*, GB4015. https://doi.org/10.1029/2004GB002221

Hwang, J., Druffel, E. R. M., & Eglinton, T. I. (2010). Widespread influence of resuspended sediments on oceanic particulate organic carbon: Insights from radiocarbon and aluminum contents in sinking particles. *Global Biogeochemical Cycles*, *24*, Gb4016. https://doi.org/10.1029/2010GB003802

Hwang, J., Druffel, E. R. M., & Komada, T. (2005). Transport of organic carbon from the California coast to the slope region: A study of Δ^{14}C and δ^{13}C signatures of organic compound classes. *Global Biogeochemical Cycles*, *19*, GB2018. https://doi.org/10.1029/2004GB002422

Hwang, J., Kim, M., Manganini, S. J., McIntyre, C. P., Haghipour, N., Park, J., et al. (2015). Temporal and spatial variability of particle transport in the deep Arctic Canada Basin. *Journal of Geophysical Research: Oceans*, *120*, 2784–2799. https://doi:10.1002/2014JC010643

Hwang, J., Manganini, S. J., Montlucon, D. B., & Eglinton, T. I. (2009). Dynamics of particle export on the Northwest Atlantic margin. *Deep-Sea Research Part I*, *56*, 1792–1803.

Hwang, J. S. J., Manganini, J., Park, D. B., Montlucon, J. M. T., & Eglinton, T. I. (2017). Biological and physical controls on the flux and characteristics of sinking particles on the Northwest Atlantic margin. *Journal of Geophysical Research: Oceans*, *122*, 4539–4553.

Jones, G. A., Gagnon, A. R., Karl, F., McNichol, A. P., & Schneider, R. J. (1994). High-precision AMS radiocarbon measurements of central Arctic Ocean sea waters. *Nuclear Instruments and Methods in Physics Research Section B: Beam Interactions with Materials and Atoms*, *92*, 426–430.

Karakaş, G., Nowald, N., Blaas, M., Marchesiello, P., Frickenhaus, S., & Schlitzer, R. (2006). High-resolution modeling of sediment erosion and particle transport across the northwest African shelf. *Journal of Geophysical Research*, *111*, C06025. https://doi.org/10.1029/2005JC003296

Kawahata, H. (2002). Suspended and settling particles in the Pacific. *Deep-Sea Research Part II*, *49*(24–25), 5647–5664.

Kawahata, H., Suzuki, A., & Ohta, H. (2000). Export fluxes in the western Pacific warm pool. *Deep-Sea Research Part I*, *47*, 2061–2091.

Kawahata, H., Yamamuro, M., & Ohta, H. (1998). Seasonal and vertical variations of sinking particle fluxes in the West Caroline Basin. *Oceanologica Acta*, *21*(4), 521–532.

Kempe, S., & Knaack, H. (1996). Vertical particle flux in the Western Pacific below the north equatorial current and the equatorial counter current. In V. Ittekkot, et al. (Eds.), *Particle Flux in the Ocean* (pp. 313–323). New York: John Wiley.

Kennicutt, M. II, Barker, C., Brooks, J., DeFreitas, D., & Zhu, G. H. (1987). Selected organic matter source indicators in the Orinoco, Nile and Changjiang deltas. *Organic Geochemistry*, *11*(1), 41–51.

Kim, M., Hwang, J., Kim, H. J., Kim, D., Yang, E. J., Ducklow, H. W., et al. (2015). Sinking particle flux in the sea ice zone of the Amundsen shelf, Antarctica. *Deep-Sea Research Part I*, *101*, 110–117.

Kim, M., Hwang, J., Lee, S. H., Kim, H. J., Kim, D., Yang, E. J., & Lee, S. (2016). Sedimentation of particulate organic carbon on the Amundsen Shelf, Antarctica. *Deep-Sea Research Part II*, *123*, 135–144.

Kim, M., Hwang, J., Rho, T., Lee, T., Kang, D.-J., Chang, K.-I., et al. (2017). Biogeochemical properties of sinking particles in the southwestern part of the East Sea (Japan Sea). *Journal of Marine Systems*, *167*, 33–42.

Kim, M., Yang, E. J., Kim, D., Jeong, J.-H., Kim, H. J., Park, J., et al. (2019). Sinking particle flux and composition at three sites of different annual sea ice cover in the Amundsen Sea, Antarctica. *Journal of Marine Systems*, *192*, 42–50.

Lam, P. J., Doney, S. C., & Bishop, J. K. (2011). The dynamic ocean biological pump: Insights from a global compilation of particulate organic carbon, $CaCO_3$, and opal concentration profiles from the mesopelagic. *Global Biogeochemical Cycles*, *25*, GB3009. https://doi.org/10.1029/2010GB003868

Lam, P. J., Ohnemus, D. C., & Auro, M. E. (2015). Size-fractionated major particle composition and concentrations from the US GEOTRACES north Atlantic zonal transect. *Deep-Sea Research Part II*, *116*, 303–320.

Liu, J. P., Liu, C. S., Xu, K. H., Milliman, J. D., Chiu, J. K., Kao, S. J., & Lin, S. W. (2008). Flux andfate of small mountainous rivers derived sediments into the Taiwan Strait. *Marine Geology*, *256*, 65–76.

Lorenzoni, L., Thunell, R. C., Benitez-Nelson, C. R., Hollander, D., Martinez, N., Tappa, E., et al. (2009). The importance of subsurface nepheloid layers in transport and delivery of sediments to the eastern Cariaco Basin, Venezuela. *Deep-Sea Research Part I*, *56*(12), 2249–2262.

Martin, J. H., Knauer, G. A., Karl, D. M., & Broenkow, W. W. (1987). VERTEX: Carbon cycling in the northeast Pacific. *Deep-Sea Research Part I*, *34*, 267–285.

Masiello, C. A., Druffel, E. R., & Bauer, J. E. (1998). Physical controls on dissolved inorganic radiocarbon variability in the California Current. *Deep Sea Research Part II*, *45*, 617–642.

McCave, I., Hall, I. R., Antia, A., Chou, L., Dehairs, F., Lampitt, R., et al. (2001). Distribution, composition and flux of particulate material over the European margin at 47°–50 °N. *Deep-Sea Research Part II*, *48*(14–15), 3107–3139.

Mollenhauer, G., Eglinton, T., Ohkouchi, N., Schneider, R., Müller, P., Grootes, P., & Rullkötter, J. (2003). Asynchronous alkenone and foraminifera records from the Benguela Upwelling System. *Geochimica et Cosmochimica Acta*, *67*(12), 2157–2171.

Nakatsuka, T., Handa, N., Harada, N., Sugimoto, T., & Imaizumi, S. (1997). Origin and decomposition of sinking particulate organic matter in the deep water column inferred from the vertical distributions of its $\delta^{15}N$, $\delta^{13}C$ and $\Delta^{14}C$. *Deep-Sea Research Part I*, *44*, 1957–1979.

Niino, H., Emery, K., & Kim, C. M. (1969). Organic carbon in sediments of Japan Sea. *Journal of Sedimentary Research*, *39*(4), 1390–1398.

Ohkouchi, N., Eglinton, T. I., Keigwin, L. D., & Hayes, J. M. (2002). Spatial and temporal offsets between proxy records in a sediment drift. *Science*, *298*, 1224.

Otosaka, S., Tanaka, T., Togawa, O., Amano, H., Karasev, E. V., Minakawa, M., & Noriki, S. (2008). Deep sea circulation of particulate organic carbon in the Japan Sea. *Journal of Oceanography*, *64*(6), 911–923.

Otosaka, S., Togawa, O., Baba, M., Karasev, E., Volkov, Y. N., Omata, N., & Noriki, S. (2004). Lithogenic flux in the Japan Sea measured with sediment traps. *Marine Chemistry*, *91*(1), 143–163.

Rea, D. K., & Hovan, S. A. (1995). Grain size distribution and depositional processes of the mineral component of abyssal sediments: Lessons from the North Pacific. *Paleoceanography*, *10*, 251–258.

Sherrell, R. M., Field, M. P., & Gao, Y. (1998). Temporal variability of suspended mass and composition in the Northeast Pacific water column: relationships to sinking flux and lateral advection. *Deep-Sea Res. II*, *45*, 733–761.

Shin, K., Noriki, S., Itou, M., & Tsunogai, S. (2002). Dynamics of sinking particles in northern Japan trench in the western North Pacific: Biogenic chemical components and fatty acids biomarkers. *Deep-Sea Research Part II*, *49*(24–25), 5665–5683.

Stuiver, M., & Polach, H. A. (1977). Discussion; reporting of C-14 data. *Radiocarbon*, *19*, 355–363.

Tagliabue, A., Bowie, A. R., DeVries, T., Ellwood, M. J., Landing, W. M., Milne, A., et al. (2019). The interplay between regeneration and scavenging fluxes drives ocean iron cycling. *Nature Communications*, *10*, 4960. https://doi.org/10.1038/s41467-019-12775-5

Taylor, S. R., & McLennan, S. M. (1985). *The Continental Crust: Its Composition and Evolution: An Examination of the Geochemical Record Preserved in Sedimentary Rocks. United States: N. p* (p. 1985). Oxford: Blackwell Scientific Publications.

Thunell, R., Benitez-Nelson, C., Varela, R., Astor, Y., & Muller-Karger, F. (2007). Particulate organic carbon fluxes along upwelling-dominated continental margins: Rates and mechanisms. *Global Biogeochemical Cycles*, *21*, GB1022. https://doi.org/10.1029/2006GB002793

Thunell, R., Tappa, E., Varela, R., Llano, M., Astor, Y., Muller-Karger, F., & Bohrer, R. (1999). Increased marine sediment suspension and fluxes following an earthquake. *Nature*, *398*(6724), 233.

Torres Valdés, S., Painter, S., Martin, A., Sanders, R., & Felden, J. (2014). Data compilation of fluxes of sedimenting material from sediment traps in the Atlantic Ocean. *Earth System Science Data*, *6*, 123–145.

Volk, T., & Hoffert, M. I. (1985). Ocean carbon pumps: Analysis of relative strengths and efficiencies in ocean-driven atmospheric CO_2 changes. In E. T. Sundquist, & V. S. Broeckcr (Eds.), *The Carbon Cycle and Atmospheric CO: Natural Variations Archean to Present*, *Geophysical Monograph Series* (Vol. 32, pp. 99–110). Washington, D.C: AGU.

Walsh, I., Fischer, K., Murray, D., & Dymond, J. (1988). Evidence for resuspension of rebound particles from near-bottom sediment traps. *Deep-Sea Research Part I*, *35*, 59–70.

Wang, X. C., Druffel, E. R. M., Griffin, S., Lee, C., & Kashgarian, M. (1998). Radiocarbon studies of organic compound classes in plankton and sediment of the northeastern Pacific Ocean. *Geochimica et Cosmochimica Acta*, *62*(8), 1365–1378.

References From the Supporting Information

Antia, A. N., von Bodungen, B., & Peinert, R. (1999). Particle flux across the mid-European continental margin. *Deep-Sea Research Part I*, *46*(12), 1999–2024.

Bathmann, U. V., Peinert, R., Noji, T. T., & Bodungen, B. V. (1990). Pelagic origin and fate of sedimenting particles in the Norwegian Sea. *Progress in Oceanography*, *24*(1–4), 117–125.

Bauerfeind, E., Nöthig, E.-M., Beszczynska, A., Fahl, K., Kaleschke, L., Kreker, K., et al. (2009). Particle sedimentation patterns in the eastern Fram Strait during 2000–2005: Results from the Arctic long-term observatory HAUSGARTEN. *Deep-Sea Research Part I*, *56*(9), 1471–1487.

Bory, A., Jeandel, C., Leblond, N., Vangriesheim, A., Khripounoff, A., Beaufort, L., et al. (2001). Downward particle fluxes within different productivity regimes off the Mauritanian upwelling zone (EUMELI program). *Deep-Sea Research Part I*, *48*(10), 2251–2282.

Bray, S., Trull, T., & Manganini, S. (2000). SAZ Project moored sediment traps: Results of the 1997–1998 deployments. *Cooperative research centre for Antarctica and the Southern Ocean* (pp. 1–127). Hobart, Australia: Antarctic Climate and Ecosystems Cooperative Research Centre (ACE CRC).

Chang, A. S., Bertram, M. A., Ivanochko, T., Calvert, S. E., Dallimore, A., & Thomson, R. E. (2013). Annual record of particle fluxes, geochemistry and diatoms in Effingham Inlet, British Columbia, Canada, and the impact of the 1999 La Niña event. *Marine Geology*, *337*, 20–34.

Dymond, J., & Lyle, M. (1985). Flux comparisons between sediments and sediment traps in the eastern tropical Pacific: Implications for atmospheric $C0_2$ variations during the Pleistocene. *Limnology and Oceanography*, *30*(4), 699–712.

Fahl, K., & Nothig, E. (2007). Lithogenic and biogenic particle fluxes on the Lomonosov Ridge (central Arctic Ocean) and their relevance for sediment accumulation: Vertical vs. lateral transport. *Deep-Sea Research Part I*, *54*(8), 1256–1272.

Helmke, P., Romero, O., & Fischer, G. (2005). Northwest African upwelling and its effect on offshore organic carbon export to the deep sea. *Global Biogeochemical Cycles*, *19*, GB4015. https://doi.org/10.1029/2004GB002265

Honda, M.C. (2001). Studies of carbon cycles in the NW Pacific Ocean by sediment trap and C14 data, *PhD thesis, Hokkaido University, Sapporo,* Japan (in 2 Parts).

Honda, M. C., Kawakami, H., Watanabe, S., & Saino, T. (2013). Concentration and vertical flux of Fukushima-derived radiocesium in sinking particles from two sites in the Northwestern Pacific Ocean. *Biogeosciences*, *10*, 3525–3534. https://doi.org/10.5194/bg-10-3525-2013

Honjo, S. (1990). Particle fluxes and modern sedimentation in the Polar Oceans. In W. O. Smith (Ed.), *Polar Oceanography, Part B: Chemistry, Biology, and Geology* (pp. 687–739). New York: Academic Press.

Honjo, S. (1996). Fluxes of particles to the interior of the open oceans. In V. Ittekkot, P. Schafer, S. Honjo, & P. J. Depetris (Eds.), *Particle Flux in the Ocean* (pp. 91–154). New York, N.Y: John Wiley & Sons.

Honjo, S., & Manganini, S. (1992). Biogenic particle fluxes at the 34°N 21°W and 48°N 21°W stations, 1989–1990: Methods and analytical data compilation. In *WHOI Technical Report* (pp. 1–77). Woods Hole, MA: WHOI.

Honjo, S., & Manganini, S. (2003). Sediment trap data, biogenic particle fluxes. In *United States JGOFS process study data 1989–1998; CD-ROM* (Vol. 1, pp. 1–77). WHOI, USA: US JGOFS Data Management Office..

Honjo, S., Manganini, S., Karowe, A. L., & Woodward, B. L. (1987). Particle fluxes, northeastern Nordic Seas: 1983–1986. In *WHOI Technical Report* (pp. 1–84). Woods Hole, MA: WHOI.

Honjo, S., & Manganini, S. J. (1993). Annual biogenic particle fluxes to the interior of the North Atlantic Ocean; studied at 34°N 21°W and 48°N 21°W. *Deep-Sea Research Part I*, *40*(1–2), 587–607.

Honjo, S., Manganini, S. J., & Wefer, G. (1988). Annual particle flux and a winter outburst of sedimentation in the northern Norwegian Sea. *Deep-Sea Research Part I*, *35*(8), 1223–1234.

Jeandel, C., Ruiz-Pino, D., Gjata, E., Poisson, A., Brunet, C., Charriaud, E., et al. (1998). KERFIX, a time-series station in the Southern Ocean: A presentation. *Journal of Marine Systems*, *17*(1–4), 555–569.

Jickells, T., Newton, P., King, P., Lampitt, R., & Boutle, C. (1996). A comparison of sediment trap records of particle fluxes from 19 to 48 °N in the northeast Atlantic and their relation to surface water productivity. *Deep-Sea Research Part I*, *43*(7), 971–986.

Jonkers, L., Brummer, G. J. A., Peeters, F. J., van Aken, H. M., & De Jong, M. F. (2010). Seasonal stratification, shell flux, and oxygen isotope dynamics of left-coiling N. pachyderma and T. quinqueloba in the western subpolar North Atlantic. *Paléo*, *25*(2), PA2204. https://doi.org/10.1029/2009PA001849

Lampitt, R., & Antia, A. N. (1997). Particle flux in deep seas: Regional characteristics and temporal variability. *Deep-Sea Research Part I*, *44*(8), 1377–1403.

Lampitt, R., Bett, B., Kiriakoulakis, K., Popova, E., Ragueneau, O., Vangriesheim, A., & Wolff, G. A. (2001). Material supply to the abyssal seafloor in the Northeast Atlantic. *Progress in Oceanography*, *50*(1–4), 27–63.

Lampitt, R., Salter, I., de Cuevas, B. A., Hartman, S., Larkin, K. E., & Pebody, C. A. (2010). Long-term variability of downward particle flux in the deep northeast Atlantic: Causes and trends. *Deep-Sea Research Part II*, *57*(15), 1346–1361. https://doi.org/10.1016/j.dsr2.2010.01.011

Lee, C., Peterson, M. L., Wakeham, S. G., Armstrong, R. A., Cochran, J. K., Miquel, J. C., et al. (2009). Particulate organic matter and ballast fluxes measured using time-series and settling velocity sediment traps in the northwestern Mediterranean Sea. *Deep-Sea Research Part II*, *56*(18), 1420–1436.

Migon, C., Sandroni, V., Marty, J.-C., Gasser, B., & Miquel, J.-C. (2002). Transfer of atmospheric matter through the euphotic layer in the northwestern Mediterranean: Seasonal pattern and driving forces. *Deep-Sea Research Part II*, *49*(11), 2125–2141.

Mohiuddin, M. M., Nishimura, A., Tanaka, Y., & Shimamoto, A. (2002). Regional and interannual productivity of biogenic components and planktonic foraminiferal fluxes in the northwestern Pacific Basin. *Marine Micropaleontology*, *45*(1), 57–82.

Mohiuddin, M. M., Nishimura, A., Tanaka, Y., & Shimamoto, A. (2004). Seasonality of biogenic particle and planktonic foraminifera fluxes: Response to hydrographic variability in the Kuroshio Extension, northwestern Pacific Ocean. *Deep-Sea Research Part I*, *51*(11), 1659–1683.

Nowald, N., Iversen, M., Fischer, G., Ratmeyer, V., & Wefer, G. (2015). Time series of in-situ particle properties and sediment trap fluxes in the coastal upwelling filament off Cape Blanc, Mauritania. *Progress in Oceanography*, *137*, 1–11.

Peinert, R., Antia, A., Bauerfeind, E., Bodungen, B. V., Haupt, O., Krumbholz, M., et al. (2001). Particle flux variability in the Polar and Atlantic biogeochemical provinces of the Nordic Seas. *The northern North Atlantic* (pp. 53–68). New York: Springer.

Pena, M., Denman, K., Forbes, J., Calvert, S., & Thomson, R. E. (1996). Sinking particle fluxes from the euphotic zone over the continental slope of an eastern boundary current region. *Journal of Marine Research*, *54*(6), 1097–1122.

10.1029/2020GB006544

Pilskaln, C., Manganini, S., Trull, T., Armand, L., Howard, W., Asper, V., & Massom, R. (2004). Geochemical particle fluxes in the Southern Indian Ocean seasonal ice zone: Prydz Bay region, East Antarctica. *Deep-Sea Research Part I*, *51*(2), 307–332.

Pudsey, C. J., & King, P. (1997). Particle fluxes, benthic processes and the palaeoenvironmental record in the Northern Weddell Sea. *Deep-Sea Research Part I*, *44*(11), 1841–1876.

Rigual-Hernández, A. S., Trull, T. W., Bray, S. G., & Armand, L. K. (2016). The fate of diatom valves in the Subantarctic and Polar Frontal Zones of the Southern Ocean: Sediment trap versus surface sediment assemblages. *Palaeogeography, Palaeoclimatology, Palaeoecology*, *457*, 129–143.

Rigual-Hernández, A. S., Trull, T. W., Bray, S. G., Cortina, A., & Armand, L. K. (2015). Latitudinal and temporal distributions of diatom populations in the pelagic waters of the Subantarctic and Polar Frontal zones of the Southern Ocean and their role in the biological pump. *Biogeosciences*, *12*, 5309–5337. https://doi.org/10.5194/bg-12-5309-2015

Romero, O., Boeckel, B., Donner, B., Lavik, G., Fischer, G., & Wefer, G. (2002). Seasonal productivity dynamics in the pelagic central Benguela System inferred from the flux of carbonate and silicate organisms. *Journal of Marine Systems*, *37*(4), 259–278.

Takahashi, K., Fujitani, N., Yanada, M., & Maita, Y. (2000). Long-term biogenic particle fluxes in the Bering Sea and the central subarctic Pacific Ocean, 1990–1995. *Deep-Sea Research Part I*, *47*(9), 1723–1759.

Takahashi, T., Fujitani, N., Yanada, M., & Maita, Y. (1997). Five year long particle fluxes in the central subarctic Pacific and the Bering Sea, in *Biogeochemical Processes in the North Pacific*, edited by Tsunogai, S., pp. 277–289, Japan Marine Science Foundation, Tokyo.

Tesi, T., Langone, L., Ravaioli, M., Giglio, F., & Capotondi, L. (2012). Particulate export and lateral advection in the Antarctic Polar Front (Southern Pacific Ocean): One-year mooring deployment. *Journal of Marine Systems*, *105*, 70–81.

Tett, Paul (2005). Flux values of different LOIS-Trap Sites. PANGAEA. https://doi.org/10.1594/PANGAEA.56170

Timothy, D., Wong, C., Barwell-Clarke, J., Page, J., White, L., & Macdonald, R. W. (2013). Climatology of sediment flux and composition in the subarctic Northeast Pacific Ocean with biogeochemical implications. *Progress in Oceanography*, *116*, 95–129.

Trull, T. W., Bray, S. G., Manganini, S. J., Honjo, S., & Francois, R. (2001). Moored sediment trap measurements of carbon export in the Subantarctic and Polar Frontal Zones of the Southern Ocean, south of Australia. *Journal of Geophysical Research*, *106*(C12), 31,489–31,509.

Turich, C., Schouten, S., Thunell, R. C., Varela, R., Astor, Y., & Wakeham, S. G. (2013). Comparison of TEX_{86} and $U_{37}^{K'}$ temperature proxies in sinking particles in the Cariaco Basin. *Deep-Sea Research Part I*, *78*, 115–133.

Walter, H., Geibert, W., van der Loeff, M. R., Fischer, G., & Bathmann, U. (2001). Shallow vs. deep-water scavenging of ^{231}Pa and ^{230}Th in radionuclide enriched waters of the Atlantic sector of the Southern Ocean. *Deep-Sea Research Part I*, *48*(2), 471–493.

Waniek, J. J., Schulz-Bull, D. E., Kuss, J., & Blanz, T. (2005). Long time series of deep water particle flux in three biogeochemical provinces of the northeast Atlantic. *Journal of Marine Systems*, *56*(3–4), 391–415.

Wefer, G., & Fischer, G. (1991). Annual primary production and export flux in the Southern Ocean from sediment trap data. *Marine Chemistry*, *35*, 597–613.

Wefer, G., & Fischer, G. (1993). Seasonal patterns of vertical particle flux in equatorial and coastal upwelling areas of the eastern Atlantic. *Deep-Sea Research Part I*, *40*(8), 1613–1645.

Wefer, G., Fischer, G., Füetterer, D., & Gersonde, R. (1988). Seasonal particle flux in the Bransfield Strait, Antartica. *Deep-Sea Research Part I*, *35*(6), 891–898.

Wefer, G., Fischer, G., Fütterer, D., Gersonde, R., Honjo, S., & Ostermann, D. (1990). Particle sedimentation and productivity in Antarctic waters of the Atlantic sector. In *Geological history of the polar oceans: Arctic versus Antarctic*, Edited (pp. 363–379). New York: Springer.

Wong, C., Whitney, F., Crawford, D., Iseki, K., Matear, R., Johnson, W., et al. (1999). Seasonal and interannual variability in particle fluxes of carbon, nitrogen and silicon from time series of sediment traps at Ocean Station P, 1982–1993: Relationship to changes in subarctic primary productivity. *Deep-Sea Research Part I*, *46*(11–12), 2735–2760.